Desalination and Water Treatment
www.deswater.com

doi: 10.5004/dwt.2022.28879

273 (2022) 172–179
October

Investigation of Pb(II) biosorption from aqueous media via *Erwinin* sp. isolated from the heavy metal-containing soils

Lei Liu[a,b], Yuxin Zhao[a], Ziqi Miao[a], Binbin Zhang[a], Wenjuan Sun[a,*], Hongzhi Wan[b,*]

[a]*School of Environment and Chemical Engineering, Anhui Vocational and Technical College, Hefei 230011, China, emails: wjsungzliang@163.com (W. Sun), liulei@cmpt.ac.cn (L. Liu), 354696149@qq.com (Y. Zhao), 2578500886@qq.com (Z. Miao), 3207718716@qq.com (B. Zhang)*

[b]*Anhui Province Key Laboratory of Medical Physics and Technology, Institute of Health and Medical Technology, Hefei Institutes of Physical Science, Chinese Academy of Sciences, Hefei 230031, China, Tel. +86 551 64689053; Fax: +86 551 64689053; email: wanghz@hfcas.ac.cn (H. Wan)*

Received 8 February 2022; Accepted 20 August 2022

ABSTRACT

This paper focuses on the potential application of *Erwinin* sp. in environmental purification. The Pb(II) biosorption was studied by batch method under different external environment (pH value, biosorption time, *Erwinin* sp. dosage, Pb(II) concentration and temperature). Batch experiments showed that *Erwinin* sp. could rapidly reach the biosorption equilibrium (90 min) of high capacity of Pb(II) biosorption (71.73 mg/g, T = 303 K) by Langmuir model. The interaction mechanism between Pb(II) and *Erwinin* sp. was investigated by TEM, XPS and FT-IR. Results of FT-IR and XPS showed that *Erwinin* sp. were rich in functional groups, which was the main reason for the effective Pb(II) removal. The Pb(II) biosorption was also studied by kinetic model and thermodynamic model. Pb(II) biosorption conforms to pseudo-second-order mode and is a spontaneous endothermic process. According to the above results, *Erwinin* sp. is a potential biosorbent for the treatment of lead pollution due to its wide source of biosorption materials, large biosorption capacity and high treatment efficiency.

Keywords: Pb(II); Biosorption; *Erwinin* sp.; Kinetic; Thermodynamic

1. Introduction

With the acceleration of industrialization in China, heavy metals such as zinc, cadmium, mercury, arsenic, lead, nickel and chromium play an important role in human production and life. The extensive application of heavy metals in the production process has brought serious heavy metal pollution to the soil [1]. Soil is an important part of ecosystem. Soil heavy metal pollution mainly comes from "three wastes" in industrial production process and some agricultural production activities [2]. Soil pollution caused by heavy metals is becoming increasingly serious [3]. It has brought a great negative impact on human health and living environment. Therefore, it is urgent to improve soil environmental quality and strengthen soil management [4]. Pb(II) is one of the most toxic heavy metals to animals, plants and human beings in the environment. Excessive biosorption of Pb by animals and plants will affect their normal growth [5,6]. Pb(II) and its compounds are non-degradable environmental pollutants, which seriously endanger human health. The damage of Pb(II) to the body is multisystem and multiorgan, including the toxic effects on bone marrow hematopoietic system, reproductive system, digestive system and other systems. As a poison of central nervous system, Pb(II) is more harmful to children's health and intelligence [7]. In addition, Pb(II) is also a carcinogen.

* Corresponding authors.

According to animal experiments and human studies on the carcinogenicity of Pb(II), the U.S. Environmental Protection Agency thinks that Pb(II) is a human carcinogen. Pb(II) in farmland soil enters the human body through agricultural products such as grains and vegetables. Positive measures must be taken to prevent and control environmental Pb(II) pollution and harm to human body.

The main treatment measures are: Physical remediation, Chemical remediation, Bioremediation [8,9]. Bioremediation is to reduce the heavy metal content in polluted soil by using biological reduction and biological purification. Compared with other methods, this treatment method has the advantages of simple operation and better remediation effect [10,11]. At present, there is not a complete method to deal with heavy metal pollution, but biological control is the direction full of application prospects. In this experiment, the adsorption effect of Pb(II) ions by *Erwinin* sp., which is separated from the polluted soil and has resistance to Pb(II), in order to explore the adsorption treatment method of heavy metal pollution different from that of plants. Compared with other similar technologies such as evaporation, chemical precipitation, activated carbon adsorption, ion exchange resin adsorption, extraction, liquid membrane and electrodialysis, microbial biosorption, as a new technology for heavy metal pollution treatment, has the advantages of wide source of biosorption materials, large adsorption capacity, good selectivity, high treatment efficiency, easy desorption and repeated adsorption [12]. Microbial biosorption refers to the use of a series of biochemical actions of microbial cells to adsorb metal or non-metal substances in aqueous solutions [13]. Amirnia uses *Saccharomyces cerevisiae* to remove Pb(II), and the mechanism of Pb(II) biosorption by living cells is cell surface adsorption and intracellular adsorption, and cell surface adsorption is the main removal mechanism [14].

The purpose of this investigation is as follows: (1) to study the interaction between Pb(II) and *Erwinin* sp. in different external environment (such as pH, biosorption time, *Erwinin* sp. dosage, Pb(II) concentration, temperature); (2) to elucidate the interaction mechanism between Pb(II) and *Erwinin* sp. by using transmission electron microscopy (TEM), Fourier transform infrared spectroscopy (FT-IR) and X-ray photoelectron spectroscopy (XPS); (3) Kinetics model and thermodynamics model were used to study the Pb(II) biosorption by *Erwinin* sp. In this study, Pb(II) biosorption was mainly carried out by using *Erwinin* sp., which was selected from soil and was resistant to lead. This study has potential application value for microbial remediation of heavy metals.

2. Materials and methods

2.1. Reagents and isolation of biosorbent

The biosorbent in the experiment was isolated from lead-contaminated soil (Feidong Recycling Industrial Park). 0.1 g of the soil polluted by heavy metals was sampled and cultured in a 100 mL conical flask. 0.2 mL of the soil suspension was taken and coated in a solid medium. Then, the bacteria were cultured in four groups of liquid medium. The content of Pb(II) in each group of medium was 50, 100, 200 and 500 mg/L for 24 h under the normal culture condition of 37°C. 5 g/L peptone, 1 g/L D-glucose and 2.5 g/L yeast extract were used in Yangji broth. The bacterial colony growing on the medium with the highest concentration of Pb(II) was selected as the strain with the highest resistance, and the strain was selected for continuous culture until a single strain appeared. The single strain was cultured in 100 mL liquid medium at 37°C for 24 h. DNA was extracted, amplified by PCR. The specific separation and identification methods refer to the study of Liu et al. [15]. Results were aligned in the NCBI database to determine the homology with the existing reference sequence [16].

2.2. Characterization methods

Erwinin sp. were investigated using Transmission electron microscope (TEM) (Hitachi S-4800) and Fourier transform infrared spectrometer (FTIR) (Thermo Scientific IS10, USA) in the wave number range 4,000–500 cm^{-1}. X-ray Photoelectron Spectroscopy (XPS) (ESCALAB250Xi, USA) was used for element analysis. Refer to the study of Liu et al. [15] for culture and preparation of *Erwinin* sp.

2.3. Batch experiments

The biosorption experiments were carried out at pH 6.0 and 0.01 mol/L KCl. Briefly, 1.0 mL of 0.5 mol/L KCl, 44.0 mL of sterile water, 5.0 mL of 600 mg/L Pb(II) stock solution and 0.1 g *Erwinin* sp. suspension (wet cells) were mixed. After 2 h of equilibration, the liquid phase was separated from solid phase by centrifuging it at 8,000 rpm for 5 min. The concentration of Pb(II) in supernatant solutions was measured by a UV-visible spectrophotometer. The biosorption percentage (R, %), biosorption capacity (Q, mg/g) and biosorption distribution coefficient (K, mL/g) are expressed as Eqs. (1)–(3), respectively:

$$R = \frac{\left(C_0 - C_e\right)}{C_0} \times 100\% \tag{1}$$

$$Q = \frac{\left(C_0 - C_e\right) \times V}{m} \tag{2}$$

$$K = \frac{\left(C_0 - C_e\right) \times V}{C_e \times m} \tag{3}$$

where C_0 and C_e (mg/L) are original and equilibrated concentration, respectively. V (mL) and m (g) are the suspension volume and the mass of biosorbent, respectively.

3. Results and discussion

3.1. Characterization

Erwinin sp. is a lead-resistant microorganism isolated from heavy metal-contaminated soil and has good biosorption performance for lead. The morphology of *Erwinin* sp. before and after Pb(II) biosorption was characterized by

TEM. Fig. 1a shows that the normal life activity of *Erwinin* sp. is strong in oval cell wall. Fig. 1b reflects that the cell wall is dissolved after Pb(II) biosorption, and the internal organelles are obviously aggregated and dissolved. The cell surface becomes more loose. Fig. 2 shows the infrared spectrum study of *Erwinin* sp. before and after Pb(II) biosorption. As shown in Fig. 2, after the Pb(II) biosorption, a new peak appeared at 800 cm^{-1}, which was considered to be the result of anti-symmetric vibration of oxygen-containing groups. The result show that *Erwinin* sp. has rich functional groups such as carboxyl, amino, phosphoryl. After Pb(II) uptake, there is also a peak (1,700 cm^{-1}), ketone carbonyl, dihydrogen linked (p-disubstituted) identification. The FT-IR also showed that the insoluble exopolysaccharides and proteins played an important role in the removal of heavy metals, especially the amide and carboxyl groups on the insoluble exoproteins were the main functional groups for the Pb(II) biosorption [17].

As previously mentioned, the microstructure of *Erwinin* sp. changed significantly before and after Pb(II) biosorption. In order to understand the Pb(II) biosorption by *Erwinin* sp., we collected and analyzed the XPS spectra of *Erwinin* sp. before and after Pb(II) biosorption. The corresponding results are shown in Fig. 3a. As can be seen from the spectrum of *Erwinin* sp., the binding energy of Pb4f appears after the absorption reaction. As shown in Fig. 3b, the Pb4f spectrum of *Erwinin* sp. has two peaks at about 139 and 143 eV, corresponding to $Pb4f_{5/2}$ and $Pb4f_{7/2}$ respectively. Combined with SEM and FTIR results, Pb(II) was adsorbed. The peaks near 139eV belong to $PbCO_3$ and $(Pb_3(OH)_2(CO_3)_2)$, while the peaks near 143 eV belong to sulfur mineral compounds [18]. As shown in Fig. 3c, the C1s spectrum was divided into peaks of about 284 eV (C–C/ C–H), 286.3 eV (C–N) and 288 eV (C=O) [19]. The O1s spectrum was divided into peaks of about 531 eV (O=C) and 532.5 eV (O–C). As shown in Fig. 3d, after Pb(II) biosorption, the peak area and binding energy position of O1s changed significantly. These changes are attributed to the formation of bonds between lead and oxygen atoms (O–Pb), which greatly affect the distribution of electrons around oxygen [20]. After Pb(II) absorption, the peak area and binding energy position of O1s changed significantly.

3.2. Effect of pH and biosorbent dosage

Fig. 4a shows pH value affects the protonation or deplasmization of the upper functional group. Based on the solubility analysis and species distribution simulation, visual minteq 3.0 is used to analyze the relationship between the distribution of Pb species in aqueous solution. As shown in Fig. 4a, Obviously, when pH < 10.0, Pb(II) ions mainly exist in the form of $PbOH^+$ and $Pb_3(OH)_4^{2+}$, and when pH > 10.0, they exist in the form of $Pb(OH)_2$. Therefore, when pH < 10.0, the increase of Pb biosorption is caused by the following two factors, electrostatic attraction between the cation of Pb(II) and the negative charge of *Erwinin* sp., with the increase of pH value, the deproton effect of cell function group is enhanced, which is conducive to the combination

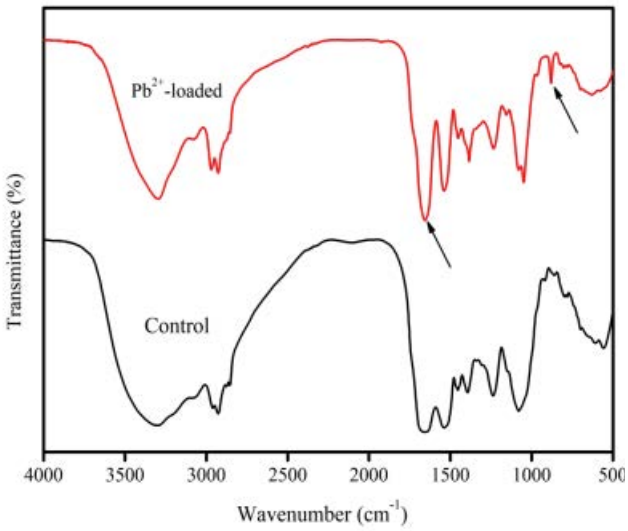

Fig. 2. FT-IR spectra of *Erwinin* sp. before and after biosorption of Pb(II).

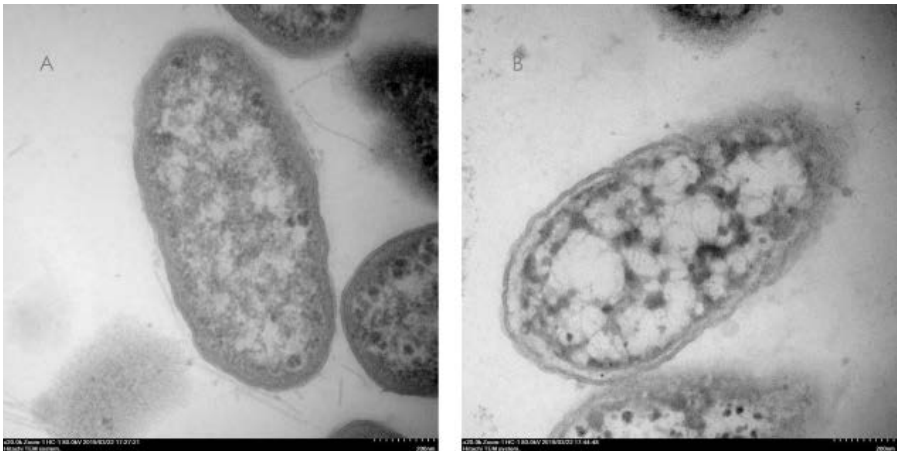

Fig. 1. TEM images of. *Erwinin* sp. (a) control and (b) loaded-Pb(II), respectively.

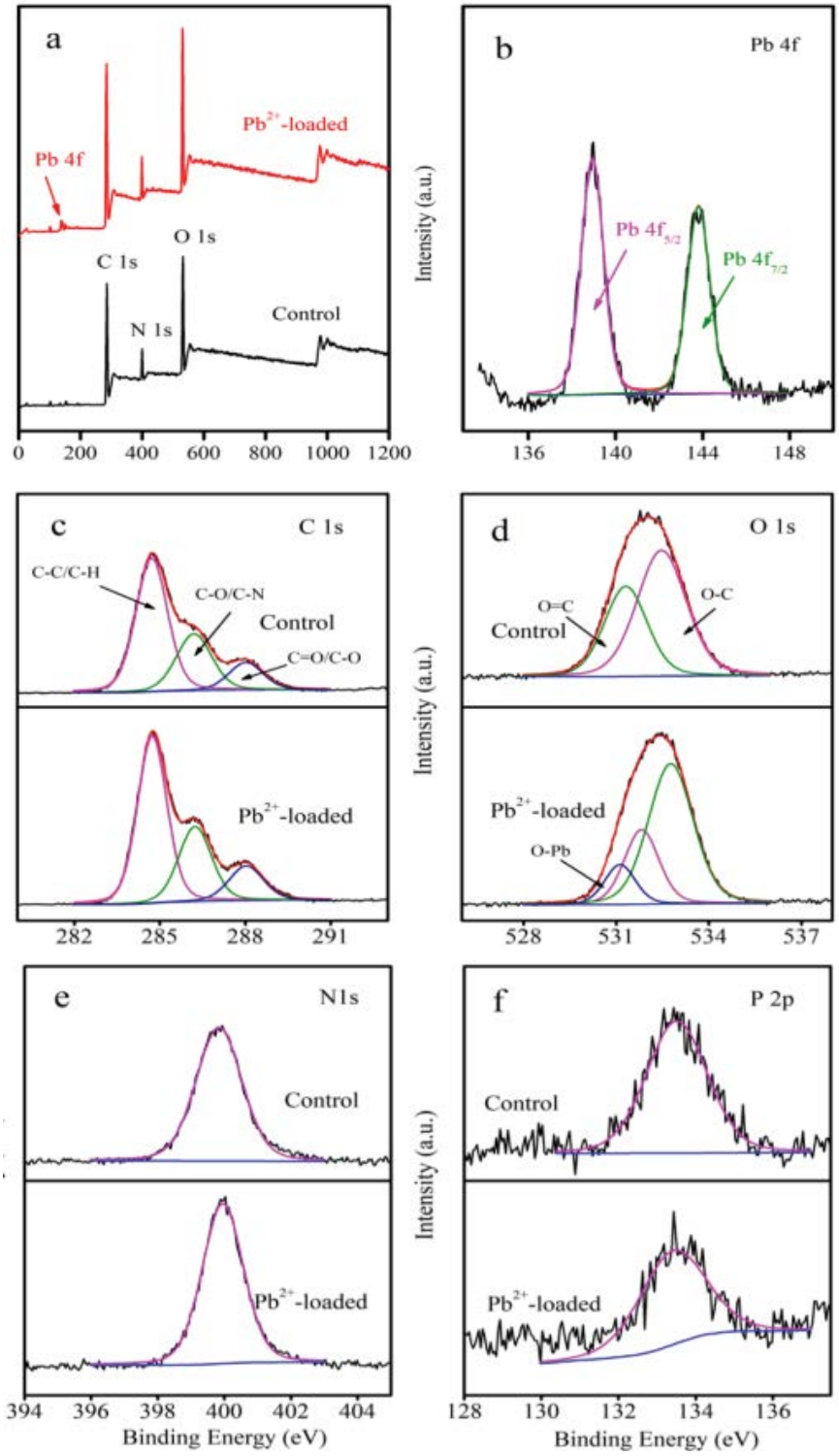

Fig. 3. XPS Intensity curves of Pb biosorption on *Erwinin* sp., (a) total survey scans, (b) Pb4f as a function of the binding energy, (c–d) C 1s,O 1s, N 1s, P 2p.

of cell and lead. However, when pH > 10.0, the biosorption rate slows down because of the electrostatic repulsion between *Erwinin* sp. [21,22].

Fig. 5 indicates the effect of the amount of biosorbent on the biosorption of lead by *Erwinin* sp. as shown in the figure, when the bacterial dosage reaches 1.1 g/L, the growth trend of biosorption rate slows down, which may be the result of bacterial cell aggregation. This aggregation reduces the effective adsorption area and enhances the interference between binding sites. That is to say, a higher amount of

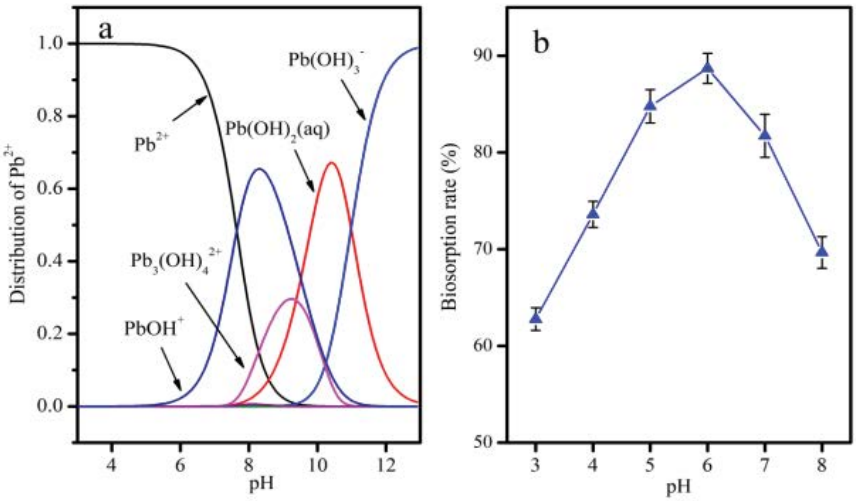

Fig. 4. (a) The relative species distribution of 60 mg/L Pb^{2+}; (b) Effect of pH on Pb(II) biosorption by *Erwinin* sp. ($C_{Pb(II)}$ = 60 mg/L, V = 50 mL, m/V = 1.0 g/L, T = 303 K, n = 3).

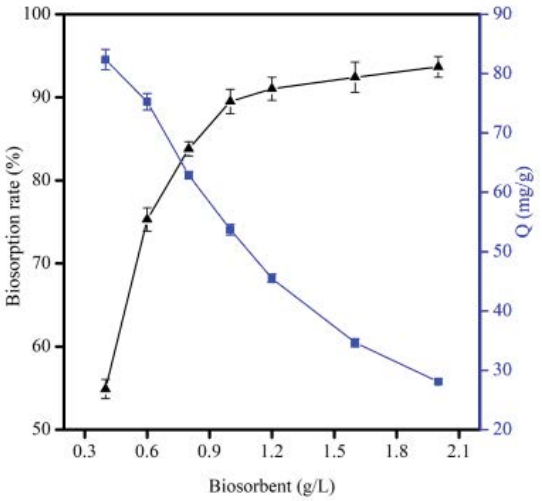

Fig. 5. The effect of biosorbent dosage on biosorption of Pb(II) by *Erwinin* sp. ($C_{Pb(II))}$ = 60 mg/L, pH = 6.0, V = 50 mL, T = 303 K, n = 3).

biosorbent has a "screening effect" on the adsorbent, which results in a slower growth trend of Pb(II) biosorption rate per unit biosorbent [23].

3.3. Biosorption isotherms

The biosorption isotherms, including the Langmuir and Freundlich isotherm models, which can reveal the surface properties of the biosorbent and the affinity to the adsorbate [24]. Langmuir and Freundlich models were showed by Eqs. (4) and (5), respectively:

$$Q_e = \frac{Q_m b C_e}{1 + b C_e} \tag{4}$$

$$Q_e = K_F C_e^{1/n} \tag{5}$$

where Q_e (mg/g) and C_e (mg/L) are the equilibrium concentration of Pb(II) at solid and solution, respectively. Q_m is the maximum biosorption capacity (mg/g), and b and K_F are Langmuir and Freundlich constant, respectively. n is the advantage of biosorption [25].

As shown in Fig. 6, the isotherms of Pb(II) biosorption on *Erwinin* sp. showed the biosorption capacity at different temperatures. According to the correlation coefficient (R^2), the Pb(II) biosorption on *Erwinin* sp. was more consistent with the Langmuir isotherm model. This result indicated that the Pb(II) biosorption was a monolayer biosorption [26]. The fitting results and relevant parameters are shown in Table 1. Based on the Langmuir isotherm model, the maximum amounts of Pb(II) biosorption (Q_m) by *Erwinin* sp. at different temperatures (293, 303 and 318 K) were 68.99, 71.73 and 72.55 mg/g, respectively. It can be found that increasing the temperature was more conducive to the enrichment of lead.

3.4. Biosorption kinetics

The pseudo-first-order, pseudo-second-order and the intra-particle diffusion models were determined by Eqs. (6)–(8):

$$Q_t = Q_e\left(1 - e^{-k_1 t}\right) \tag{6}$$

$$Q_t = \frac{k_2 Q_e^2 t}{1 + k_2 Q_e t} \tag{7}$$

$$Q_t = k_i t^{1/2} + c \tag{8}$$

where Q_t is biosorption capacity at time t, and Q_e (mg/g) is biosorption capacity at equilibrium, k_1 (min^{-1}) and k_2 (g/mg·min) are the equilibrium constants, respectively.

Fig. 7a reflects the relationships between the time and the biosorption capacity of *Erwinin* sp. for Pb(II). The

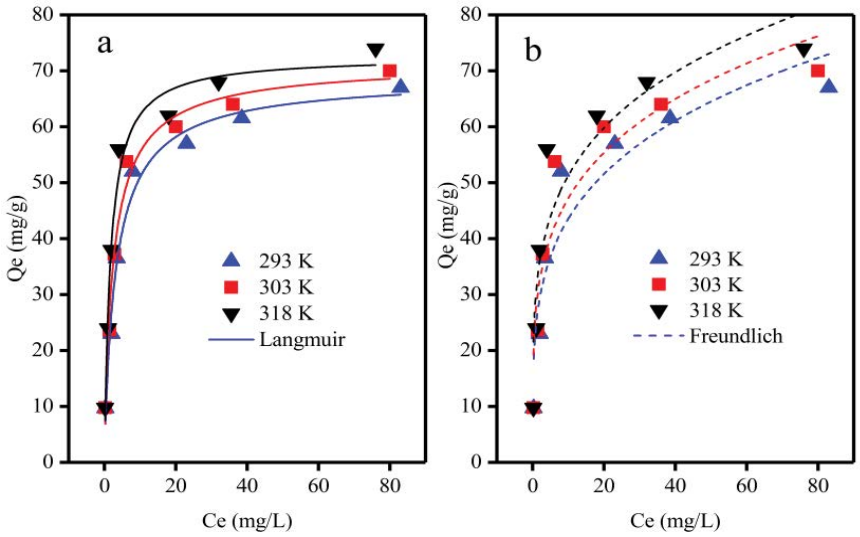

Fig. 6. Biosorption isotherms (a) Langmuir model (b) Freundlich model ($C_{Pb(II)}$ = 60 mg/L, pH = 6.0, V = 50 mL, T = 303 K).

Table 1
Parameters for the Langmuir and Freundlich isotherm models

T (K)	Langumir			Freundlich		
	Q_m	b	R^2	K_F	n	R^2
293	68.99	0.337	0.974	24.86	0.244	0.872
303	71.73	0.443	0.978	27.79	0.230	0.861
318	72.55	0.582	0.981	30.78	0.221	0.846

biosorption capacity of Pb(II) increased rapidly in the first 60 min, then slowly increased, and finally reached equilibrium in 90 min. The biosorption kinetics, including pseudo-first-order, pseudo-second-order and Weber–Morris intraparticle diffusion kinetic models. The fitting results and relevant parameters are shown in Table 2. The result indicates the time for *Erwinin* sp. to reach equilibrium in the Pb(II) biosorption, which was used to evaluate the speed of the biosorption process. As shown in Fig. 7b–d, according to the correlation coefficient (R^2), the Pb(II) biosorption on *Erwinin* sp. was more consistent with pseudo-second-order than pseudo-first-order kinetic. This result indicated the biosorption process was mainly controlled by chemical adsorption or ion exchange [27]. Fig. 7c is a Weber–Morris model of internal diffusion dynamics. The entire biosorption process consists of three stages. The first stage is the fast biosorption stage, the second stage is the slow diffusion stage, and the third stage is the adsorption equilibrium stage [28].

3.5. Thermodynamic parameter analysis

The thermodynamic analysis (standard Gibbs free energy change $\Delta G°$, standard enthalpy change $\Delta H°$ and standard entropy change $\Delta S°$) are shown by Eqs. (9) and (10), respectively:

$$\ln K = \frac{\Delta H°}{RT} + \frac{\Delta S°}{R} \tag{9}$$

$$\Delta G° = \Delta H° - T\Delta S° \tag{10}$$

where R and T are gas constants (8.314 J/(mol·K)) and Kelvin temperature, respectively. Relationship curve between $\ln(Q_e/C_e)$ and $1/T$ of Erwinin sp.

The values of $\Delta H°$ and $\Delta S°$ can be calculated by the intercept and slope of linear Eq. (8), respectively. As shown in Table 3, the change of Gibbs free energy of Pb(II) bioaccumulation in *Erwinin* sp. at three temperatures (293, 303 and 318 K) is –4.7, –5.61 and –6.98 kJ/mol, respectively. The results show that the biosorption process of lead was spontaneous

Table 2
Kinetic parameters of Pb(II) biosorption on *Erwinin* sp.

Kinetic model	T (K)	k_1 (min^{-1})/k_2 (g/mg·min) k_i (mg/g·min$^{-1/2}$)	Q_e (mg/g) C_i (mg/g)	R^2
Pseudo-first-order	303	0.0259	19.93	0.951
Pseudo-second-order	303	0.0025	56.02	0.999
W–M model	303	4.075	18.51	0.948
		2.159	33.23	0.980
		0.020	54.72	0.881

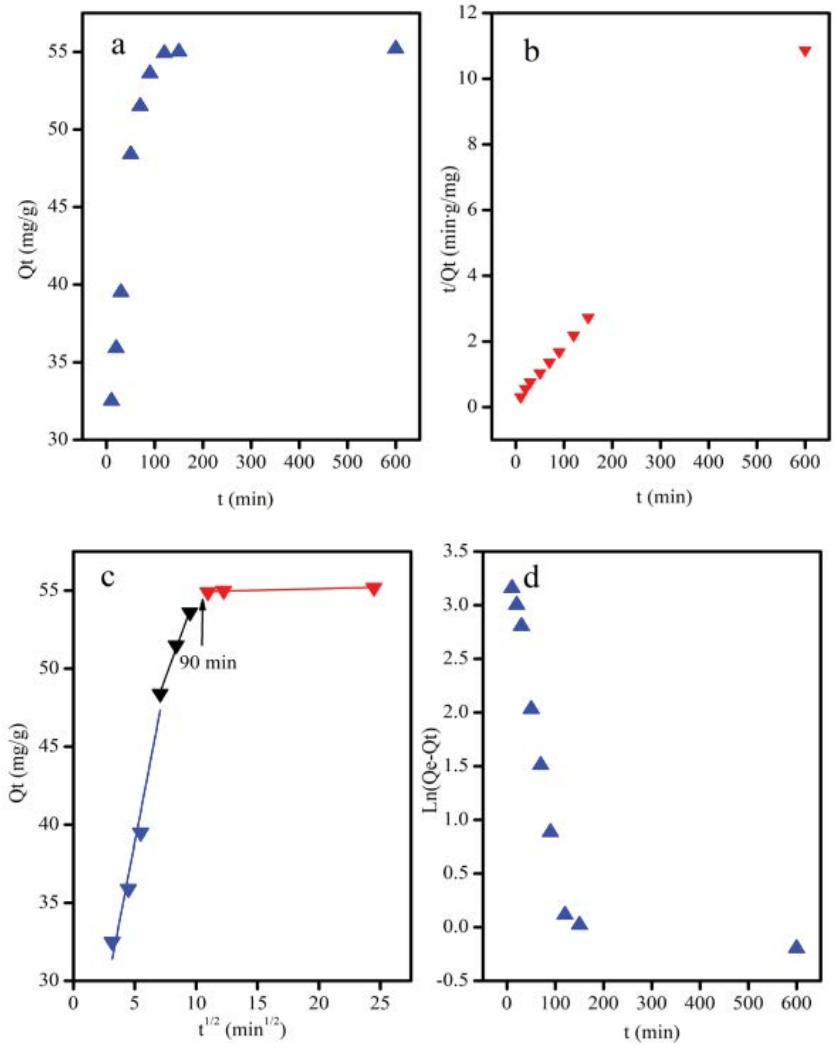

Fig. 7. (a) The biosorption kinetics of *Erwinin* sp. on Pb(II), (b) pseudo-second-order model, (c) Weber–Morris intraparticle diffusion kinetic models and (d) pseudo-first-order model (m/V = 1.0 g/L, $C_{Pb(II)}$ = 60 mg/L, T = 303 K, pH = 6.0).

Table 3
Thermodynamic parameters for Pb biosorption on *Erwinin* sp.

T (K)	$\Delta G°$ (kJ/mol)	$\Delta H°$ (kJ/mol)	$\Delta S°$ (J/(mol·K))	R^2
293	–4.70			
303	–5.61	22.04	91.26	0.990
318	–6.98			

[29,30]. The $\Delta H°$ indicates the biosorption process was endothermic in nature, which is clear from the Q_m values that increase with an increase in temperature [30]. According to the thermodynamic analysis, increasing the temperature is beneficial to the biosorption of heavy metals, which has certain guiding significance for practical application.

4. Conclusion

The mechanism of Pb(II) biosorption by *Erwinin* sp. was investigated by TEM, XPS and FT-IR. Batch tests showed that *Erwinin* sp. could rapidly reach the biosorption balance

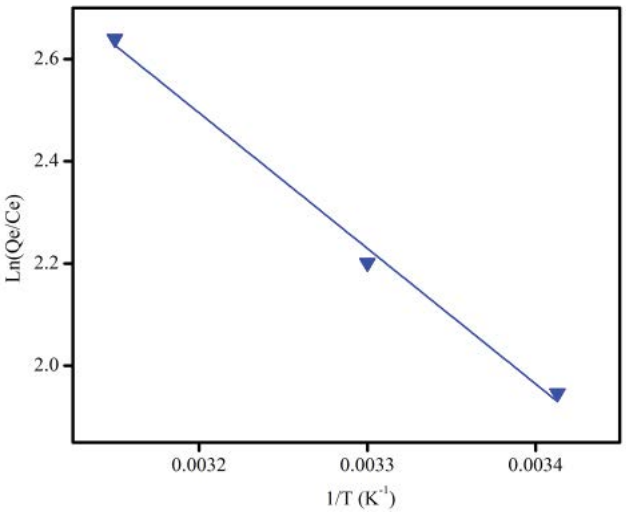

Fig. 8. Relationship curve between $\ln(Q_e/C_e)$ and $1/T$ of *Erwinin* sp. (m/V = 1.0 g/L, $C_{Pb(II)}$ = 60 mg/L, T = 303 K, pH = 6.0.

(90 min) of high biosorption capacity (71.73 mg/g, 303 K). FT-IR and XPS analysis showed that *Erwinin* sp. were rich in functional groups and responsible for the effective of Pb(II) uptake, and Pb(II) biosorption was independent of the ionic strength, which showed the formation of spheroid surface. These results also indicated that *Erwinin* sp. can be considered as a potential biosorbent for lead removal.

Conflicts of interest

All authors declare that they have no actual or potential conflicts.

Acknowledgement

This study was supported by the Anhui Province University Natural Science Research Project (KJ2018A0709, KJ2021A1447, KJ2021A1448), Key projects of Anhui province university outstanding youth talent support program (gxyqZD2021144), Scientific research project of Anhui Vocational and Technical College (azy2020KJ05).

References

[1] S. Cheng, Heavy metal pollution in China: origin, pattern and control, Environ. Sci. Pollut. Res., 10 (2003) 192–198.
[2] M. Halim, P. Conte, A. Piccolo, Potential availability of heavy metals to phytoextraction from contaminated soils induced by exogenous humic substances, Chemosphere, 52 (2003) 265–275.
[3] O.J. Afonne, E.C. Ifediba, Heavy metals risks in plant foods-need to step up precautionary measures, Curr. Opin. Toxicol., 22 (2020) 1–6.
[4] D. Damodaran, K.V. Shetty, B.R. Mohan, Effect of chelaters on bioaccumulation of Cd(II), Cu(II), Cr(VI), Pb(II) and Zn(II) in *Galerina vittiformis* from soil, Int. Biodeterior. Biodegrad., 85 (2013) 182–188.
[5] C. Zhang, K. Yang, Y. Li, F. Cheng, K. Rong, Spectral characteristics and the study of pollution degree of maize leaves under copper and lead stress, J. Indian Soc. Remote Sens., 48 (2020) 21–33.
[6] R. Musielińska, J. Kowol, J. Kwapuliński, R. Rochel, Antagonism between lead and zinc ions in plants, Arch. Environ. Prot., 42 (2016) 78–91.
[7] J. Marta, G. Anna, V. Franck, Modelling assisted phytoremediation of soils contaminated with heavy metals – main opportunities, limitations, decision making and future prospects, Chemosphere, 249 (2020) 126196, doi: 10.1016/j.chemosphere.2020.126196.
[8] M. Soleimani, T. Kaghazchi, Adsorption of gold ions from industrial wastewater using activated carbon derived from hard shell of apricot stones-an agricultural waste, Bioresour. Technol., 99 (2008) 5374–5383.
[9] M. Bobik, I. Korus, L. Dudek, The effect of magnetite nanoparticles synthesis conditions on their ability to separate heavy metal ions, Arch. Environ. Prot., 43 (2017) 3–9.
[10] J.K. Jensen, P.E. Holm, J. Nejrup, M.B. Larsen, O. K. Borggaard, The potential of willow for remediation of heavy metal polluted calcareous urban soils, Environ. Pollut., 157 (2009) 931–937.
[11] M. Thomas, B. Bialecka, D. Zdebik, Removal of copper, nickel and tin from model and real industrial wastewater using sodium trithiocarbonate. The negative impact of complexing compounds, Arch. Environ. Prot., 44 (2018) 33–47.
[12] B. Pourrut, S. Jean, J. Silvestre, E. Pinelli, Lead-induced DNA damage in *Vicia faba* root cells: potential involvement of oxidative stress, Mutat. Res., 726 (2011) 123–128.
[13] T.A. Saleh, M. Tuzen, A. Sar, Magnetic activated carbon loaded with tungsten oxide nanoparticles for aluminum removal from waters, J. Environ. Chem. Eng., 5 (2017) 2853–2860.
[14] S. Amirnia, M.B. Ray, A. Margaritis, Heavy metals removal from aqueous solutions using *Saccharomyces cerevisiae* in a novel continuous bioreactor-biosorption system, Chem. Eng. J., 264 (2015) 863–872.
[15] L. Liu, J. Liu, X.T. Liu, C.W. Dai, Z.X. Zhang, W.C. Song, Kinetic and equilibrium of U(VI) biosorption onto the resistant bacterium *Bacillus amyloliquefaciens*, J. Environ. Radioact., 203 (2019) 117–124.
[16] A. Esposito, F. Pagnanelli, A. Lodi, C. Solisio, F. Vegliò, Biosorption of heavy metals by *Sphaerotilus natans*: an equilibrium study at different pH and biomass concentrations, Hydrometallurgy, 60 (2001) 129–141.
[17] R.M. Gabr, S.H.A. Hassan, A.A.M. Shoreit, Biosorption of lead and nickel by living and non-living cells of *Pseudomonas aeruginosa* ASU 6a, Int. Biodeterior. Biodegrad., 62 (2008) 195–203.
[18] X. Xu, X. Hu, Z. Ding, Y. Chen, B. Gao, Waste-art-paper biochar as an effective sorbent for recovery of aqueous Pb(II) into value-added PbO nanoparticles, Chem. Eng. J., 308 (2017) 863–871.
[19] E. Abu-Danso, S. Peräniemi, T. Leiviskä, A. Bhatnagar, Synthesis of S-ligand tethered cellulose nanofibers for efficient removal of Pb(II) and Cd(II) ions from synthetic and industrial wastewater, Environ. Pollut., 242 (2018) 1988–1997.
[20] X. Yin, X. Meng, Y. Zhang, W. Zhang, H. Sun, J.T. Lessl, Removal of V(V) and Pb (II) by nanosized TiO_2 and ZnO from aqueous solution, Ecotoxicol. Environ. Saf., 164 (2018) 510–519.
[21] H.O. Zhang, W.Z. Zhou, Y.H. Ma, H.X. Zhao, Y.Z. Zhang, FTIR spectrum and detoxication of extracellular polymeric substances secreted by microorganism, Spectrosc. Spect. Anal., 33 (2013) 3041–3043.
[22] Y.L Li, Y.N. Wei, S.Q. Huang, X.S. Liu, Z.H. Jin, Z. Meng, Biosorption of Cr(VI) onto *Auricularia auricula* dreg biochar modified by cationic surfactant: characteristics and mechanism, J. Mol. Liq., 269 (2018) 824–832.
[23] J. Tang, L. Zhang, J. Zhang, L. Ren, Y. Zhou, Y. Zheng, L. Luo, Y. Yang, H. Huang, A. Chen, Physicochemical features, metal availability and enzyme activity in heavy metal-polluted soil remediated by biochar and compost, Sci. Total Environ., 701 (2019) 134751, doi: 10.1016/j.scitotenv.2019.134751.
[24] J. Zhang, Y. Sun, Molecular cloning, expression and characterization of a chitosanase from *Microbacterium* sp., Biotechnol. Lett., 29 (2007) 1221–1225.
[25] Z.M. Jin, L. Xia, Z. Tuo, L.J. Liu, T. Black, K.C. Jones, H. Zhang, X. Wang, N. Jin, D. Zhang, Interrogating cadmium and lead biosorption mechanisms by *Simplicillium chinense* via infrared spectroscopy, Environ. Pollut., 263 (2020) 114419, doi: 10.1016/j.envpol.2020.114419.
[26] L. Liu, M.Y. Xia, J.W. Hao, H. X. Xu, W.C. Song, Biosorption of Pb(II) by the resistant *Enterobacter* sp.: investigated by kinetics, equilibrium and thermodynamics, Arch. Environ. Prot., 47 (2021) 28–36.
[27] S. Deng, T. Ke, L. Li, S. Cai, Y. Zhou, Y. Liu, Impacts of environmental factors on the whole microbial communities in the rhizosphere of a metal-tolerant plant: *Elsholtzia haichowensis* sun, Environ. Pollut., 237 (2018) 1088–1097.
[28] C.E.R. Barquilha, E.S. Cossicha, C.R.G. Tavares, E.A. Silva, Biosorption of nickel(II) and copper(II) ions by *Sargassum* sp. in nature and alginate extraction products, Bioresour. Technol. Rep., 5 (2019) 43–50.
[29] H. Beheshti, M. Irani, Removal of lead(II) ions from aqueous solutions using diatomite nanoparticles, Desal. Water Treat., 57 (2016) 18799–18805.
[30] A.S. Bhatt, P.L. Sakaria, M. Vasudevan, R.R. Pawar, N. Sudheesh, H.C. Bajaj, Adsorption of an anionic dye from aqueous medium by organoclays: equilibrium modeling, kinetic and thermodynamic exploration, RSC Adv., 2 (2012) 8663–8671.